

11CNIT-XX-2018 FULLPAPER

INTERCONVERSION BETWEEN DIELECTRIC AND MECHANICAL MEASUREMENTS OF POLYMERIC MATERIALS FOR WIND TURBINE COATINGS

**B. Pascual-Jose¹, A. Ribes-Greus^{1, *}, Fernando Sánchez², Antonio Falcó², Enrique
Cortés³**

¹ Technical Institute of Materials (ITM), Polytechnic University of Valencia (UPV), Camí de Vera s/n,
46022 Valencia, Spain.

² ESI Chair at CEU-UCH, Departamento de Matemáticas, Física y Ciencias Tecnológicas, Universidad
Cardenal Herrera-CEU, CEU Universities, 46115 Moncada-Valencia, Spain.

³ AEROX Advanced Polymers, 46185 Poble Vallbona-Valencia, Spain.

*e-mail (corresponding author): aribes@ter.upv.es

ABSTRACT

The trend in the wind energy sector is to build wind turbines with longer blades that causes a significant increase in the nominal tip speed. This means that the leading edge is now exposed to higher stresses that end up damaging it. As a result, the performance and the Annual Energy Production (AEP) are reduced. In addition, a higher operational cost, due mainly to inspection and repairing costs, makes leading edge erosion (LEE) one of the main challenges for the wind energy sector.

Among the factors causing the LEE the most important is the atmospheric environment. A detailed study of rain-induced erosion shows that the damage is produced by the propagation of the shock-waves generated after the impact. These shock-waves do not only affect the outer layer of the leading edge protection (LEP) but the entire multi-layer system. Therefore, to solve this problem, the elastic and viscoelastic response as well as the interaction between the layers of the different polymeric materials used must be studied. To that purpose a mechanical test of the materials employed in the construction of the LEP is required.

The Dynamic Mechanical Thermal Analysis (DMTA) is the appropriate technique to determine the viscoelastic properties. However, the information provided by this technique is only valid up to a frequency of 10^2 Hz, and therefore, it is not useful in the present context. On the other hand, Dielectric Thermal Analysis (DETA) supplies information on the molecular motion up to a frequency of 10^7 Hz. Thus, the aim of this work was to obtain relevant mechanical data by means of measuring the complex dielectric permittivity (ϵ^*) over the entire frequency range and converting it to the complex Young modulus (E^*). To that end, a series of mathematical models capable of performing such interconversion were applied and evaluated.

Keywords: Leading edge erosion; Wind turbine coatings; Dynamic Mechanical Thermal Analysis (DMTA); Dielectric Thermal Analysis (DETA); Interconversion of mechanical and dielectrical relaxations;

1. Introduction

Wind energy is probably the most promising renewable source of energy. In recent years, this sector has experienced a notable growth. For instance, in the 1990s the current average onshore turbine capacity was 1 MW while nowadays it has increased up to 3 MW (Bartolomé, Teuwen 2018). Governmental policies have induced the energy industry to move towards a scenario where sustainable sources of energy provide a high percentage of the energetic demand so that nuclear energy and fossil fuels can eventually be completely replaced (Paris Agreement 2015). To that purpose, the wind energy sector must increase its annual energy production (AEP). The most feasible manner to meet this increment in the energetic demand is to augment the offshore production by means of installing larger turbines. However, this increment in size comes at a price. It has been estimated that these new turbines with larger blades will have tip speeds over 110 m/s (Cortés et. al. 2017). Therefore, at these speeds, rain induced erosion becomes an even more serious problem since it damages the protective coating surrounding the blades. Thus, it is expected to increase the operation and maintenance costs as well as to decrease the AEP, up to a 27% according to some estimations (Eisenberg et. al. 2018), due to the profile change caused by the delamination process (Bech et. al. 2018). Research in this field is still in development due to the complexity of the physical mechanisms and the lack of proper test rigs that accurately assess this damage (Bartolomé, Teuwen 2018). Accordingly, new studies introducing novel designs of test rigs are being developed to provide accurate and reproducible measurements (O'Carroll et. al. 2018; Gaunaa et. al. 2018; Fraisse et. al. 2018; Zhang et. al. 2015; Liersch, Michael 2014; Keegan et. al. 2013), together with computational studies describing the physics of rain erosion testers in an effort to understand how these test rigs erode the sample (Gaunaa et. al. 2018). In addition, new analytical and computational models are being developed to describe the physics of water droplet impingement accurately (Eisenberg et. al. 2018; Amirzadeh et. al. 2017a, 2017b). It is expected that the outcome of this research will facilitate the creation of new industrial standards that will improve and facilitate the design, test and validation of new coating materials that provide a better performance under erosive conditions.

Leading edge erosion (LEE) is defined as the erosion caused by the impact of water droplets on the leading edge of a wind turbine blade. A way to quantify the degree of erosion is to account for the loss of mass produced on the coating's surface. To that purpose, three different stages are found. The initial stage is called the incubation period where the effects of erosion are hardly noticeable since only small variations on the superficial roughness occur. After this stage the first cracks are spotted on the coating surface. It is at this stage when the loss of mass becomes measurable. If no measures are taken, the cracks continue to grow until delamination occurs. These series of events are usually reflected in an erosion curve. The stresses responsible of the erosion process after the impact are propagated through a series of shock waves. More precisely, the impact of the droplet on the coating's surface generates three different wave fronts. The first one is due to the normal stress generated after the impact that is transmitted across the entire surface of the blade through a longitudinal compressional wave. In addition, the shear stresses originate a transverse wave that is transmitted across the entire surface of the blade as well. Finally, a Rayleigh wave is generated due to the deformation of the droplet itself. However, this wave is confined to the region near the impact (Valaker et. al. 2015).

To determine properly the physics of the water droplet impingement on the coated surface it is necessary to study the viscoelastic properties. To that end, the appropriate methodology to study

the viscoelastic properties by means of the Dynamic Mechanical Thermal Analysis (DMTA). Nevertheless, since the frequencies of impact have been estimated to be in the range of $10^5 - 10^7$ Hz, the information provided by this technique is not useful a priori since the desired frequency range is not covered. The present work, thus, introduces a new approach consisting of applying the dielectric broadband spectroscopy (DBS), that covers a wide frequency range, and then to perform the interconversion between viscoelastic and dielectric data by means of a mathematical model. More precisely, the DiMarzio Bishop model (DMB) (DiMarzio, Bishop 1974) is able to perform the interconversion using only the data obtained from the DBS, whereas the model presented in (Garcia-Bernabé et. al. 2009) combines the information obtained from DBS and DMTA to perform the interconversion. Both methods are applied to a dataset from Poly lactide acid (PLA) samples and their performance is assessed.

2. Materials and methodology

The sample material used in this work is Poly Lactic Acid (PLA). PLA is a biodegradable thermoplastic with a glass temperature transition (T_g) located around 45-65 °C. Furthermore, it presents high mechanical strength, good thermal properties and low environmental impact. The data corresponding to both dielectric and mechanical spectra are obtained from the work presented in (Badia et. al. 2012; Badia et. al. 2014).

Dielectric broadband and Dynamic Mechanical spectra possess characteristic peaks that can be compared due to their similarities (McCrum et. al. 1967). The DiMarzio-Bishop (DMB) model relates the complex dielectric permittivity (ϵ^*) to the complex shear modulus (G^*) by means of Eq. 1.

$$\frac{\epsilon^* - \epsilon_\infty}{\epsilon_0 - \epsilon_\infty} = \frac{1}{1 + K G^*(\omega)} \quad (1)$$

where k is the Boltzmann constant, T is the temperature, K is the DB parameter, ϵ_∞ and ϵ_0 are the unrelaxed and relaxed permittivity respectively. To obtain this relationship the model assumes a dynamic viscosity (η^*), i.e., a frequency dependent viscosity.

The second model considered in this work is the interconversion algorithm developed by A. Garcia-Bernabé et.al., hereinafter referred to as AGB model. This model uses two different viscosities, rotational and translational, arising from the dielectric and mechanical contributions respectively. Therefore, the interconversion between dielectric and mechanical data is performed using a power law relation between these viscosities. The final conversion between the complex dielectric permittivity and the dynamic shear modulus is done by means of Eq. 2.

$$G_s^*(\omega\delta) - G_0 = \left[\frac{\epsilon_0 - \epsilon_\infty}{\epsilon^*(\omega) - \epsilon_\infty} - 1 \right]^{\frac{1}{a\zeta}} \frac{\delta^c}{B/K} \frac{1}{(i\omega)^{\left(\frac{1}{\zeta} - c\right)}} \quad (2)$$

Where, B is a scale factor, ζ is a shape factor, δ is a shift factor, K is the DB parameter, the exponents a and c are fractional exponents related to the rotational and translational viscosity respectively.

3. Results and discussion

The analysis of both dielectric and mechanic spectra was conducted essentially through the imaginary parts of the complex dielectric permittivity (ϵ'') and the complex Young's modulus (E'') respectively. The relaxation times were found using the empirical Havriliak-Negami (HN) equation (Havriliak, Negami 1966), as shown in Eq. 3.

$$\epsilon''(\omega) - \epsilon_\infty = \sum_k \text{Im} \left[\frac{\Delta\epsilon}{\{(1 + (i\omega\tau_{HN})^{\alpha_k})\}^{\beta_k}} \right] \quad (3)$$

where α_k and β_k are parameters corresponding to the width and asymmetry of the relaxation time distributions, respectively; τ_{HN} is the Havriliak-Negami relaxation time, and k represents the number of the individual HN contributions, which usually varies from $k = 1$ to 3, depending on the complexity of the ϵ'' .

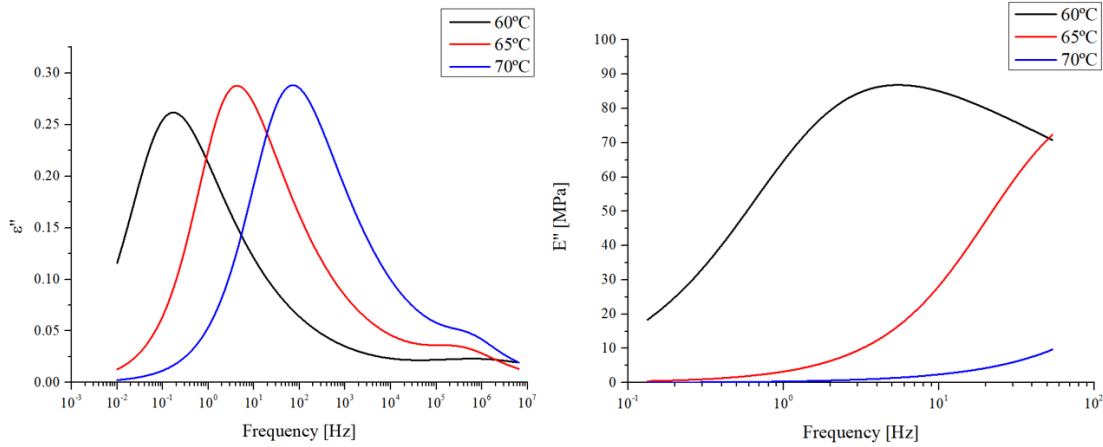


Figure 1 HN curves for the imaginary part of the complex permittivity (Left). HN curves for the imaginary part of the complex Young Modulus (Right).

The resultant equations for both dynamic and mechanic spectra are shown in **Figure 1**. Note that the fitting was done in order to obtain a good resolution of the α relaxation that is associated to the glass transition. The short range covered by dynamic mechanical analysis does not allow to observe the complete relaxation processes, specially at 65 and 70 °C, although both can be inferred.

The DMB model provided reasonable values for the storage Young's modulus (E') up to a frequency of 10^5 Hz. For higher frequencies it was found that the curves diverged. In Figure 2 it is shown that the range of values of E' are highly influenced by the value of the DB parameter. This term depends on the values of the relaxed (ϵ_0) and unrelaxed (ϵ_∞) permittivity. In addition, since most viscoelastic solids present a thermorheologically complex behaviour the strength parameter would not be constant anymore, i.e. it does not fulfil the Time-Temperature-Superposition (TTS). Therefore, K varies with temperature as well. This difference is shown in Table 1 and it might not seem significant at low temperatures, but it becomes greater as temperature increases.

Table 1 Value of the DB parameter at different temperatures.

Temperature	K_1	K_2
60 °C	2.34×10^{-7}	3.66×10^{-9}
65 °C	2.35×10^{-7}	3.67×10^{-9}
70 °C	2.37×10^{-7}	3.70×10^{-9}

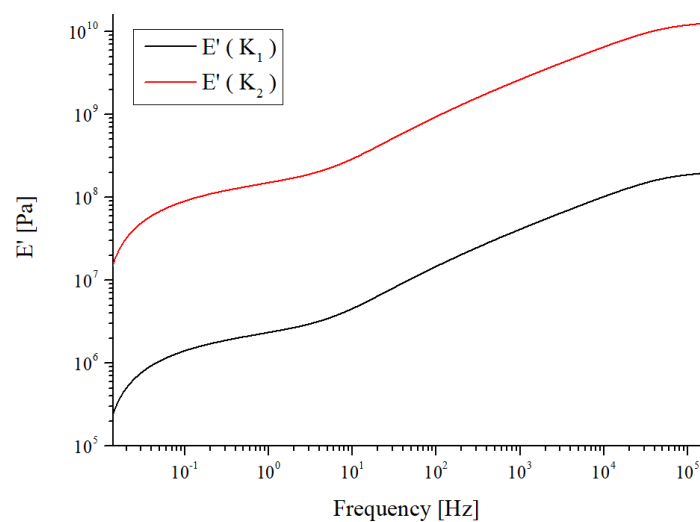


Figure 2 Storage Young modulus obtained with the DMB model for 70 °C.

Overall, it was found that the model captures well the alpha relaxation. This is of paramount importance since a material used as a leading edge protector (LEP) is expected to work in the rubber like state to absorb as much energy from the impacts as possible, thus increasing its life cycle. However, the main issue with this model is that the values are as accurate as the value chosen for the DB parameter.

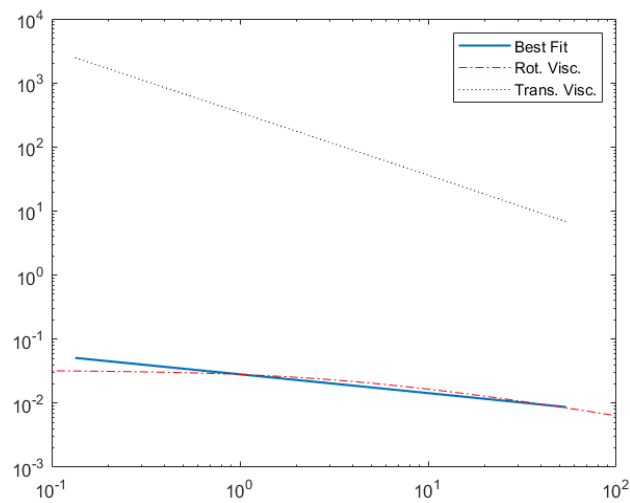


Figure 3 Best fit for Eq.5 for a temperature of 70 °C.

Figure 3 shows the rotational and translational viscosities as well as the best fit for the AGB model. The obtained results are as expected. Note that the translational viscosity was obtained from DMTA data, and therefore, only a short range of values ($10^{-1} - 10^2$ Hz) are calculated. The AGB model, is only valid for the α relaxation, and thus, the temperatures used when determining the values of the viscosities were 60 °C, 65 °C and 70 °C. The values for the fitting parameters are shown in Table 2 and were obtained using a nonlinear least square fitting algorithm.

Table 2 Fitting parameters for Eq. 5 and the high frequency value for the storage Young's modulus.

Temperature	Log(B)	δ	ξ	E_{∞}' [MPa]
60°C	-0.9694	0.0186	0.9624	285
65°C	-2.3042	0.0184	0.5687	2015
70°C	-3.6948	0.0169	0.4634	-

Originally this model was validated in glass former liquids and the shear modulus was determined using a piezoelectric transducer which reaches higher frequencies than a dynamic mechanical analyser. Hence, a better fit was found. However, our findings suggest that the model is still valid for viscoelastic solids although careful attention in the fitting process must be taken. In Table 2 the high frequency value (E_{∞}') is presented for the three temperatures analysed. The results indicate reasonable values for PLA. Note that the high frequency limit for 70 °C is not included because a high value was found, meaning that at those frequencies and for that temperature the PLA would have yielded. The values of the numerical shear strength modulus were found to depend as well on the value of the DB parameter.

4. Conclusions

In this work two different mathematical models to convert dielectric to mechanical data are evaluated. Originally both models were derived assuming thermorheologically simple behaviour, i.e. only one relaxation. However, in this work its applicability to model a viscoelastic solid with thermorheologically complex behaviour using dielectric broadband spectroscopy and dynamic mechanical analysis has been studied.

It was found that the DMB model is describing well the α relaxation. Therefore, it can be ascertained that it is providing a good qualitative description of the physics it is describing. However, on a quantitative point of view, the values of the storage Young's modulus are highly influenced by the value of the DB parameter.

The AGB model was evaluated considering only the α relaxation, and therefore, it disregarded all other relaxations. Nonetheless, it was found that the model provided reasonable values for both, translational and rotational, viscosities. The final conversion to shear strength modulus or storage Young's modulus was found to be highly dependent as well on the value of K , although reasonable values were found. Nonetheless, this model should be the most complete since it counts with input data coming from both, dielectric broadband spectroscopy and dynamic mechanical analysis.

5. Acknowledgements

The authors would like to thank the support of the European Union through the European Regional Development Funds (ERDF) and the Spanish Ministry of Science, Innovation and Universities, for the research project, POLYDECARBOCELL (ENE2017-86711-C3-1-R).

6. References

AMIRZADEH, B., LOUHGHALAM, A., RAESSI, M. and TOOTKABONI, M., 2017a. A computational framework for the analysis of rain-induced erosion in wind turbine blades, part II: Drop impact-induced stresses and blade coating fatigue life. *Journal of Wind Engineering and Industrial Aerodynamics*. 2017. Vol. 163, no. February, p. 44–54.

AMIRZADEH, B., LOUHGHALAM, A., RAESSI, M. and TOOTKABONI, M., 2017b. A computational framework for the analysis of rain-induced erosion in wind turbine blades, part I: Stochastic rain texture model and drop impact simulations. *Journal of Wind Engineering and Industrial Aerodynamics*. 2017. Vol. 163, no. November 2016, p. 33–43.

BADIA, J. D., STRÖMBERG, E., KARLSSON, S. and RIBES-GREUS, A., 2012. Material valorisation of amorphous polylactide. Influence of thermo-mechanical degradation on the morphology, segmental dynamics, thermal and mechanical performance. *Polymer Degradation and Stability*. 2012. Vol. 97, no. 4, p. 670–678.

BADIA, J D, MONREAL, L, SÁENZ DE JUANO-ARBONA, V and RIBES-GREUS, A, 2014. Dielectric spectroscopy of recycled polylactide. *Polymer Degradation and Stability*. 2014. Vol. 107, p. 21–27.

BARTOLOMÉ, Luis and TEUWEN, Julie, 2018. Prospective challenges in the experimentation of the rain erosion on the leading edge of wind turbine blades. *Wind Energy*. 2018. No. March. DOI 10.1002/we.2272.

BECH, Jakob I, HASAGER, Charlotte B and BAK, Christian, 2018. Extending the life of wind turbine blade leading edges by reducing the tip speed during extreme precipitation events. . 2018. No. February, p. 1–35.

CORTÉS, E, SÁNCHEZ, F, O'CARROLL, A, MADRAMANY, B, HARDIMAN, M and YOUNG, T M, 2017. On the material characterisation of wind turbine blade coatings: The effect of interphase coating-laminate adhesion on rain erosion performance. *Materials*. 2017. Vol. 10, no. 10.

DIMARZIO, Edmund A. and BISHOP, Marvin, 1974. Connection between the macroscopic electric and mechanical susceptibilities. *The Journal of Chemical Physics*. 1974. Vol. 3802, no. 1974, p. 3802–3811.

EISENBERG, Drew, LAUSTSEN, Steffen and STEGE, Jason, 2018. Wind turbine blade coating leading edge rain erosion model: Development and validation. *Wind Energy*. 2018. Vol. 21, no. January, p. 942–951.

FRAISSE, Anthony, BECH, Jakob Ilsted, BORUM, Kaj Kvisgaard, FEDOROV, Vladimir, FROST-JENSEN JOHANSEN, Nicolai, MCGUGAN, Malcolm, MISHNAEVSKY, Leon and KUSANO, Yukihiro, 2018. Impact fatigue damage of coated glass fibre reinforced polymer laminate. *Renewable Energy*. 2018. Vol. 126, p. 1102–1112.

GARCIA-BERNAB, A., SANCHIS, M. J., DÍAZ-CALLEJA, R. and DEL CASTILLO, L. F., 2009. Fractional Fokker-Planck equation approach for the interconversion between dielectric and mechanical measurements. *Journal of Applied Physics*. 2009. Vol. 106, no. 1.

GAUNAA, M, SORENSEN, N N, FROST-JENSEN JOHANSEN, N, OLSEN, A S, BAK, C and ANDERSEN, R B, 2018. Investigation of droplet path in a rain erosion tester. *Journal of Physics: Conference Series*. 2018. No. 1037.

HAVRILIAK, S and NEGAMI, S, 1966. A complex plane analysis of α -dispersions in some polymer systems. *Journal of Polymer Science Part C: Polymer Symposia*. 1966. Vol. 14, no. 1, p. 99–117.

KEEGAN, M. H., NASH, D. H. and STACK, M. M., 2013. On erosion issues associated with the leading edge of wind turbine blades. *Journal of Physics D: Applied Physics*. 2013. Vol. 46, no. 38.

LIERSCH, J. and MICHAEL, J., 2014. Investigation of the impact of rain and particle erosion on rotor blade aerodynamics with an erosion test facility to enhancing the rotor blade performance and durability. *Journal of Physics: Conference Series*. 2014. Vol. 524, no. 1.

MCCRUM, Norman Gerard, READ, Bryan Eric and WILLIAMS, Graham, 1967. *Anelastic and dielectric effects in polymeric solids*. Wiley New York.

O'CARROLL, A., HARDIMAN, M., TOBIN, E. F. and YOUNG, T. M., 2018. Correlation of the rain erosion performance of polymers to mechanical and surface properties measured using nanoindentation. *Wear*. 2018. Vol. 412–413, no. June, p. 38–48.

PARIS AGREEMENT, 2015. United nations framework convention on climate change. *Paris, France*. 2015.

VALAKER, E. A., ARMADA, S. and WILSON, S., 2015. *Droplet erosion protection coatings for offshore wind turbine blades*. Elsevier B.V.

ZHANG, Shizhong, DAM-JOHANSEN, Kim, BERNAD, Pablo L. and KIIL, Søren, 2015. Rain erosion of wind turbine blade coatings using discrete water jets: Effects of water cushioning, substrate geometry, impact distance, and coating properties. *Wear*. 2015. Vol. 328–329, p. 140–148.